

DUSTY GALAXIES AND THE DEGENERACY BETWEEN THEIR DUST DISTRIBUTIONS AND THE ATTENUATION FORMULA

KYLE PENNER¹, MARK DICKINSON², BENJAMIN WEINER³, HANAE INAMI², JEYHAN KARTALTEPE², JANINE PFORR⁴,
HOOSHANG NAYYERI⁵, SUSAN KASSIN⁶, CASEY PAPOVICH⁷, AND ALEXANDRA POPE⁸

Draft version March 5, 2022

ABSTRACT

Do spatial distributions of dust grains in galaxies have typical forms, as do spatial distributions of stars? We investigate whether or not the distributions resemble uniform foreground screens, as commonly assumed by the high-redshift galaxy community. We use rest-frame infrared, ultraviolet, and H α line luminosities of dust-poor and dusty galaxies at $z \sim 0$ and $z \sim 1$ to compare measured H α escape fractions with those predicted by the Calzetti attenuation formula. The predictions, based on UV escape fractions, overestimate the measured H α escape fractions for all samples. The interpretation of this result for dust-poor $z \sim 0$ galaxies is that regions with ionizing stars have more dust than regions with nonionizing UV-emitting stars. Dust distributions for these galaxies are nonuniform. The interpretation of the overestimates for dusty galaxies at both redshifts is less clear. If the attenuation formula is inapplicable to these galaxies, perhaps the disagreements are unphysical; perhaps dust distributions in these galaxies are uniform. If the attenuation formula does apply, then dusty galaxies have nonuniform dust distributions; the distributions are more uniform than they are in dust-poor galaxies. A broad range of H α escape fractions at a given UV escape fraction for $z \sim 1$ dusty galaxies, if real, indicates diverse dust morphologies and the implausibility of the screen assumption.

1. INTRODUCTION

A galaxy's morphology is often defined as its spatial distribution of stars. Rest-frame optical images of galaxies show diverse arrangements of their stellar components: smooth ellipticals, tightly-wound spirals, clumpy disks, barred disks, train-wrecks, fuzzballs, and whatever Willman 1 is (Willman et al. 2005, 2011). Little more than spatial extent is known about distributions of dust in dusty galaxies (Younger et al. 2010; Díaz-Santos et al. 2010; Simpson et al. 2015). Yet spatial distributions of all galactic components have intrinsic value. If we want to learn about galaxies, morphology should be a wavelength-independent word. Surprises surely abound: for example, galaxies at $z \sim 0.3$ have dust out to several Mpc. Their average dust mass profile is a constant fraction of their average halo mass profile (Ménard et al. 2010, see also Zaritsky 1994).

Dust attenuates a galaxy's intrinsic luminosity at ultraviolet (UV) and optical wavelengths. To recover an intrinsic luminosity from an emergent luminosity we often assume that dust grains are distributed as a uniformly thick screen between us and the galaxy's stars

(Calzetti et al. 1994). From the uniform screen assumption follows an attenuation formula that depends solely on wavelength.

An attenuation formula is denoted $k(\lambda)$ or $k'(\lambda)$. It differs from an extinction formula, which is independent of the spatial distribution of dust. When we derive an extinction formula, it is valid for the small area surrounding a star in the Milky Way, not the large area containing a mixture of stars in distant galaxies.

If we write this equation:

$$L_{\text{emergent}}/L_{\text{intrinsic}} = 10^{-A/2.5} = 10^{-E(B-V)k(\lambda)/2.5}$$

we assume a uniform screen not because $k(\lambda)$ is solely dependent on wavelength, but because $L_{\text{emergent}}/L_{\text{intrinsic}}$ is solely dependent on wavelength. In an illustrative sense $L_{\text{emergent}}/L_{\text{intrinsic}}$ is an attenuation formula convolved with a spatial distribution of dust.

The uniform screen assumption is unrealistic. A low-redshift galaxy with a high emergent UV luminosity and a low IR luminosity—a dust-poor galaxy—has a high UV escape fraction. The Calzetti et al. (2000) formula predicts its H α escape fraction; the prediction overestimates the measured H α escape fraction. The galaxy's regions with $> 10 M_{\odot}$ stars, which ionize gas, have more dust than its regions with less massive stars that emit in the UV and leave the gas unionized (Calzetti et al. 1994; Calzetti 1997b). While the discrepancy in amounts of dust does not invalidate the screen part of our assumption, it does invalidate the uniform part.

The screen part of our assumption is suspect, but it may be a good approximation to the truth—the alternative assumption being that dust mixes with stars. Liu et al. (2013) study the dust distribution of M83 at a spatial scale of 6 pc. They divide M83 into a center and outskirts. For each part, they calculate the percentage of regions with ionizing stars mixed with dust. Only in the

kdpenner@gmail.com

¹Laboratoire AIM, DSM/Irfu/Sap, CEA-Saclay, 91191 Gif-sur-Yvette, France

²National Optical Astronomy Observatory, Tucson, AZ 85719, USA

³Department of Astronomy, University of Arizona, Tucson, AZ 85721, USA

⁴Laboratoire d'Astrophysique de Marseille, Aix Marseille Université, 13388 Marseille cedex 13, France

⁵Department of Physics & Astronomy, University of California Irvine, Irvine, CA 92697, USA

⁶Space Telescope Science Institute, Baltimore, MD 21218, USA

⁷Department of Physics & Astronomy, Texas A&M University, College Station, TX 77843, USA

⁸Department of Astronomy, University of Massachusetts Amherst, Amherst, MA 01003, USA

center does this percentage exceed 50. If they degrade the spatial resolution to 100 pc, they conclude that the dust distribution around ionizing stars is a screen. The screen assumption is qualitatively similar to a scenario in which dust is distributed in a large number of clumps (Calzetti et al. 1994). If we choose to think of dust distributions as clumpy, the number of clumps surrounding nonionizing UV-emitting stars in low-redshift dust-poor galaxies is 60% of the number of clumps surrounding ionizing stars (Calzetti 1997a).

The discrepancy between the uniform assumption and real dust distributions in low-redshift dust-poor galaxies grows even larger if we consider that galaxies have centers and outskirts—that galaxies are not point sources. A number of studies find that H α and UV escape fractions increase with increasing radius (Boissier et al. 2004; Prescott et al. 2007; Muñoz-Mateos et al. 2009). Ionizing stars are surrounded by more dust than nonionizing UV-emitting stars; ionizing stars at large radii have less dust than ionizing stars at small radii, and similarly for nonionizing UV-emitting stars.

We know little about dust distributions in low-redshift dusty galaxies, which have high IR luminosities and low-to-high emergent UV luminosities. Their IR emitting regions span a range of sizes, from sub- to several kpc (Díaz-Santos et al. 2010). Measuring a size is hard enough; imaging a distribution is even harder. If a dusty galaxy’s measured H α escape fraction agreed with the prediction from the Calzetti et al. (2000) attenuation formula, we might conclude that the galaxy has a uniform dust distribution only if we believe that the prediction is valid. If a dusty galaxy’s measured H α escape fraction disagreed with the prediction from the Calzetti et al. (2000) formula, the galaxy might have a nonuniform dust distribution, like that of a dust-poor galaxy. This explanation for the disagreement is not unique. The galaxy might have a uniform distribution and obey a different $k(\lambda)$.

We have nothing more than vague and conflicting ideas of dust distributions in all high-redshift galaxies. Onodera et al. (2010), Kashino et al. (2013), and Price et al. (2013) argue for nonuniform distributions in their samples, which comprise dusty and dust-poor galaxies; Erb et al. (2006) present evidence for uniform distributions in a similarly mixed sample. Reddy et al. (2015) argue that the uniformity of the dust distribution depends on the galaxy’s star formation rate: as the star formation rate increases the dust distribution becomes less uniform.

In this paper, we ask the question, For dusty galaxies at $z \sim 0$ and $z \sim 1$, how do H α escape fractions relate to the predictions made by the Calzetti et al. (2000) attenuation formula? We: (1) show that H α escape fractions differ from the prediction; (2) show that the relations between H α and UV escape fractions differ from the relation for low-redshift dust-poor galaxies; and (3) argue that an interpretation in the context of dust distributions relies on the shaky assumption that the Calzetti et al. (2000) attenuation formula is universally valid.

For this paper we assume a cosmology with $H_0 = 70$ km s $^{-1}$ Mpc $^{-1}$, $\Omega_m = 0.3$, and $\Omega_\Lambda = 0.7$. Our terminology is: (1) a *uniform* screen is a screen equally thick between a region with stars which ionize gas and a region with stars which emit in the UV and do not ionize gas;

(2) a *dust-poor* galaxy generally has high values of UV and H α escape fractions; and (3) a *dusty* galaxy is selected from an IR image and generally has low values of UV and H α escape fractions. The samples of dust-poor and dusty galaxies are not dichotomous. More details are in the following section.

2. DATA

Measured and derived quantities are in Tables 2 and 3.

2.1. Measured quantities

We use IR, emergent UV, and H α luminosities to determine escape fractions. In this section we detail our catalogs and samples.

2.1.1. Sample of dusty galaxies at $z > 0.7$

Our study uses observations of the GOODS-S, COSMOS, and UDS regions. A catalog of *Herschel*/PACS 100 μ m sources for GOODS-S comes from Magnelli et al. (2013); for COSMOS and UDS, we use catalogs produced for the *Herschel* survey of CANDELS regions (Inami et al., in prep). A 100 μ m source is defined as a $\geq 3\sigma$ flux density measurement from PSF fitting to a *Spitzer*/MIPS 24 μ m source, which is based on an IRAC 3.6 μ m source prior. In GOODS-S, the catalog has flux densities at 24, 70, 100, and 160 μ m; in COSMOS and UDS, the catalogs have flux densities at 24, 100, 160, 250, 350, and 500 μ m. All flux densities are $\geq 3\sigma$. We do not use the 250, 350, and 500 μ m flux densities in the COSMOS and UDS catalogs, to avoid the effects of source confusion on PSF fitting. Including them changes our results negligibly.

We associate each 100 μ m source with a 1.6 μ m (*H*-band) source in the catalogs produced by CANDELS (Nayyeri et al., in prep; Galametz et al. 2013; Guo et al. 2013). Each catalog has broadband flux densities at many wavelengths, not all of which are common to the other two. We require the 1.6 μ m source to be a unique match within 0.7'' of the position of the 100 μ m source’s 3.6 μ m prior. The match radius is an estimate for maximizing the number of unique matches while minimizing the number of multiple matches.

The final quantity of interest for each matched source is an H α line flux or flux limit. These come from our reduction of observations from the *HST*/WFC3-IR grism survey 3D-*HST* (Brammer et al. 2012). We match each 100 μ m source to a counterpart in the direct image accompanying the grism observations. Two people in our group visually inspect the counterpart’s spectrum and then review and reconcile any discrepant redshift assignments. The H α line falls in the grism’s wavelength range for galaxies at $0.7 < z < 1.5$. The spectra have low enough wavelength resolution that the H α and [N II] lines are blended; we assume that the line flux of [NII] at $\lambda = 0.6583$ μ m is 0.3 times the H α line flux and that the line flux of [N II] at $\lambda = 0.6548$ μ m is 0.1 times the H α line flux. The ratio of [N II] to H α line fluxes depends on gas-phase metallicity so these values may be incorrect for some star-forming galaxies. The values will be correct for a significant fraction of galaxies in our sample if the sample has a distribution of gas-phase metallicity similar to that of low-redshift galaxies (Kauffmann et al. 2003).

The values will be correct for a larger fraction of galaxies in our sample if the sample has a distribution of gas-phase metallicity similar to that of low-redshift galaxies which are luminous in the near-IR (Weiner et al. 2007). For each 1D spectrum with a visible and uncontaminated line complex, we fit a linear model to the continuum and Gaussian profiles to the emission lines and extract the H α line flux. The uncertainty on the line flux comes from the covariance matrix times the fit’s reduced χ^2 . We replace $< 5\sigma$ H α line fluxes with limits. We multiply the line fluxes and limits by 1.1 as an aperture correction.

Some sources will be at $0.7 < z < 1.5$ but will not have visible H α line flux. To determine line flux upper limits for these sources, we match each $100\ \mu\text{m}$ source to a source with a spectroscopic redshift in the catalogs of: Le Fèvre et al. (2004); Szokoly et al. (2004); Mignoli et al. (2005); Yamada et al. (2005); Ravikumar et al. (2007); Vanzella et al. (2008); Lilly et al. (2009); Balestra et al. (2010); Fadda et al. (2010); Simpson et al. (2012); Kurk et al. (2013); Santini et al. (2014); Simpson et al. (in prep.); Almaini et al. (in prep.); and M. Dickinson (private communication). Operationally both the $100\ \mu\text{m}$ and spectroscopic catalogs are matched to the CANDELS catalogs. If the $100\ \mu\text{m}$ source has a spectroscopic redshift that is unconfirmed by an uncontaminated grism spectrum, we estimate the widths of the invisible Gaussian line profiles from the ratio of integrated flux density to peak surface brightness for the region of the direct image surrounding the galaxy. The direct image is the image taken as part of the grism observations. We then fit the same model as above to the 1D spectrum and extract the H α line flux uncertainty. We use 5σ limits. We are unable to determine limits for galaxies observed by the grism that are undetected in the direct image. Most limits are in GOODS-S because the spectroscopic completeness is higher there than it is in COSMOS or UDS.

To summarize, our high-redshift sample contains galaxies with: (1) detected emission at $100\ \mu\text{m}$; (2) detected emission at $1.6\ \mu\text{m}$; and (3) spectroscopically-determined redshifts at $0.7 < z < 1.5$.

2.1.2. Samples of dust-poor and dusty galaxies at $z < 0.2$

We use a nonstandard method to determine H α escape fractions, so we test this method first for low-redshift dust-poor galaxies which have known dust properties. We choose a sample of star-forming galaxies at $z \sim 0$ that are analogs of common star-forming galaxies at high redshift (LBAs; Overzier et al. 2009, 2011).

We use $24\ \mu\text{m}$ flux densities in the *Spitzer* Heritage Archive. Of the 26 sources in Overzier et al. (2011), 3 have unreliable $24\ \mu\text{m}$ flux densities per the recommendations in the enhanced imaging products quick start guide; these sources are excluded. The remaining 23 galaxies have flux densities at 0.15 and $0.23\ \mu\text{m}$ (NUV and FUV bands), from *GALEX* observations. H α line fluxes, from SDSS observations, are from Overzier (private communication). We multiply the line fluxes by 1.67 as a fiber-aperture correction (Overzier et al. 2009).

We also apply our method to a sample of low-redshift dusty galaxies, which have relatively unknown dust properties. Hwang & Geller (2013) collate, for low-redshift dust-obscured galaxies (DOGs) and a control sample: flux densities at 9, 12, 22, 25, 60, 100, and $140\ \mu\text{m}$,

from *IRAS*, *AKARI*, and *WISE* observations; 0.15 and $0.23\ \mu\text{m}$ flux densities, from *GALEX* observations; and H α line fluxes, from SDSS observations. The fiber-aperture corrections for the H α line fluxes come from the differences, in the accompanying $0.62\ \mu\text{m}$ (*r*-band) images, between Petrosian flux densities and flux densities in apertures with equal size to the fiber apertures.

2.2. Derived quantities

In this section we detail how we estimate total IR and emergent UV luminosities, UV continuum power-law indices, and star formation rates for the galaxies in our samples.

2.2.1. IR luminosities

We estimate a total IR luminosity ($8\text{--}1000\ \mu\text{m}$; L_{IR}) for each galaxy. We redshift the Chary & Elbaz (2001) template spectral energy distributions (SEDs) to the distance of each galaxy. If the galaxy has one measured IR flux density, we find the SED that most closely matches that flux density and multiply the IR luminosity of the SED by the ratio between actual and predicted flux densities. If the galaxy has two or more measured IR flux densities, we introduce a multiplicative factor f for each SED. We find the best-fit f for each SED; the result is an f and χ^2 value. We choose the SED and its accompanying f that results in the minimum of all χ^2 values. The galaxy’s L_{IR} is then f times the IR luminosity of the SED. In practice, all the high- and low-redshift dusty galaxies have two or more measured IR flux densities, and all the low-redshift dust-poor galaxies have one measured IR flux density.

Overzier et al. (2011), in their footnote 14, find that the Chary & Elbaz (2001) SEDs do not fit low-redshift dust-poor galaxies as well as other SEDs. They measured IR flux density limits at 70 and $160\ \mu\text{m}$ as well as flux densities at $24\ \mu\text{m}$. The footnote explains that the Chary & Elbaz (2001) SEDs, when fit to $24\ \mu\text{m}$ flux densities, predict flux densities at 70 and $160\ \mu\text{m}$ that fall above their upper limits. Our IR luminosities are high compared to theirs—on average, a factor of 1.4 times higher; at most, a factor of 2.5 times higher. We present results for both sets of IR luminosities for the low-redshift dust-poor galaxies.

IR luminosities are between 5×10^{10} and $1 \times 10^{12} L_{\odot}$ for the central 95% of the sample of high-redshift dusty galaxies; between 7×10^{10} and $4 \times 10^{11} L_{\odot}$ for the low-redshift dusty galaxies; and between 4×10^{10} and $5 \times 10^{11} L_{\odot}$ for the low-redshift dust-poor galaxies.

2.2.2. UV continuum power-law indices and luminosities

For galaxies with UV emission from newly formed massive stars the continuum between 0.125 and $0.263\ \mu\text{m}$ is approximately a power law with index β :

$$S_{\lambda} = C\lambda^{\beta} \quad (1)$$

where S_{λ} is flux density and λ is wavelength. We use all measured flux densities and uncertainties in this rest-frame wavelength range to fit for β and the constant factor C or for their limits. Measured flux densities may be negative—the sky aperture may be brighter than the galaxy aperture—which complicates our fitting procedure. When a galaxy has only two measured flux densities in the wavelength range, the solution for β and C

is analytic, so for a solution to exist the flux densities must be positive. If they both are, we make no cuts on their signal-to-noise ratio (S/N). If the only positive flux density, among multiple measurements, is $> 3\sigma$, we calculate a β limit using that flux density and a 3σ limit for another in the rest-frame wavelength range. Whether the limit is an upper or lower one depends on whether the detected flux density’s wavelength is lower or higher than the limit’s wavelength. We do not estimate a β limit when the only positive flux density, among multiple measurements, is $< 3\sigma$. If more than two measured flux densities are positive, regardless of their S/N and whether the surplus measurements are negative or positive, we minimize χ^2 .

We estimate an emergent UV luminosity or a limit at rest-frame $0.16\ \mu\text{m}$ for each galaxy using its redshift and the power-law fit to the rest-frame UV flux densities. We refer to the luminosity as $0.16 \times L_{0.16}$.

2.2.3. Star formation rates

The equations in Kennicutt (1998) relate IR, emergent UV, and emergent $\text{H}\alpha$ luminosities to star formation rates (SFRs). We assume that a galaxy’s total SFR: (1) is the sum of its IR- and emergent UV-derived SFR; and (2) equals the intrinsic (not emergent) $\text{H}\alpha$ -derived SFR. The SFR equations are valid under different assumptions for the duration of a galaxy’s star formation episode. Our assumptions will not conflict with those of Kennicutt (1998) if: (1) the SFR has been constant for $\sim 10^8$ yr, so that the instantaneous $\text{H}\alpha$ -derived SFR equals the prolonged UV- and IR-derived SFRs; and (2) the dominant source for the IR luminosity is not old stars or an active nucleus.

We must exclude galaxies with active nuclei because fractions of their IR, emergent UV, and emergent $\text{H}\alpha$ luminosities will be unrelated to newly formed massive stars. We identify 5 AGN hosts among the high-redshift dusty galaxies; we use the Donley et al. (2012) criteria, which are based on mid-IR flux densities, which all 3 CANDELS catalogs have. These criteria will miss some AGN hosts (Juneau et al. 2013). We accept the contaminants because in some fields we lack data—for example, X-ray data—that we could use to identify the missed AGN hosts.

Among the low-redshift dusty galaxies, we keep only those identified as star-forming by Hwang & Geller (2013). They use rest-frame optical line flux ratios to discriminate between an AGN host and a star-forming galaxy without an AGN. None of the low-redshift dust-poor galaxies host an AGN (Overzier et al. 2011).

3. RESULTS

Three star formation rates allow us to compare two attenuation values. We eschew magnitude attenuation in favor of the escape fraction, which is the ratio of emergent to intrinsic luminosity. We define the following quantities.

- $f_{\text{esc}}(0.16\ \mu\text{m})$ is the escape fraction at rest-frame $0.16\ \mu\text{m}$. In relation to A_{UV} , $f_{\text{esc}}(0.16\ \mu\text{m}) = 10^{-A_{\text{UV}}/2.5}$.
- $f_{\text{esc}}(\text{H}\alpha)$ is the escape fraction of the $\text{H}\alpha$ line luminosity.

- $f_{\text{esc}}(0.66\ \mu\text{m})$ is the escape fraction extrapolated from $f_{\text{esc}}(0.16\ \mu\text{m})$ to the wavelength of $\text{H}\alpha$ —the attenuation formula prediction. For the attenuation formula in Calzetti et al. (2000), $f_{\text{esc}}(0.66\ \mu\text{m}) = f_{\text{esc}}(0.16\ \mu\text{m})^{0.33}$.

Calzetti et al. (1994) argue that, in low-redshift dust-poor galaxies, regions with ionizing stars are spatially separate from regions with nonionizing UV-emitting stars. In this framework $f_{\text{esc}}(0.66\ \mu\text{m})$ is the escape fraction of the $0.66\ \mu\text{m}$ continuum emission from low-to-high mass stars and $f_{\text{esc}}(\text{H}\alpha)$ is the escape fraction of the $0.66\ \mu\text{m}$ line emission from gas ionized by high mass stars. These galaxies have $f_{\text{esc}}(\text{H}\alpha) = f_{\text{esc}}(0.16\ \mu\text{m})^{0.69}$, equivalent to $f_{\text{esc}}(\text{H}\alpha) = f_{\text{esc}}(0.66\ \mu\text{m})^{2.1}$ (Calzetti et al. 1994; Calzetti 1997b). Because the ionizing and nonionizing stars are spatially separate, the escape fractions disagree because the dust distributions are nonuniform. The ionizing stars are surrounded by more dust than are the nonionizing stars.

The $\text{H}\alpha$ escape fractions in Calzetti et al. (1994) come from the ratios of $\text{H}\alpha$ to $\text{H}\beta$ line luminosities. In the absence of dust the ratio is 2.86, so $(L_{\text{H}\alpha}/L_{\text{H}\beta})/2.86 = f_{\text{esc}}(\text{H}\alpha)/f_{\text{esc}}(\text{H}\beta)$. Since $f_{\text{esc}}(\text{H}\beta)$ is a power-law function of $f_{\text{esc}}(\text{H}\alpha)$, the ratio of line luminosities uniquely determines $f_{\text{esc}}(\text{H}\alpha)$.

The UV and $0.66\ \mu\text{m}$ escape fractions in Calzetti et al. (1994) come from comparing spectra of galaxies with $\text{H}\alpha$ escape fractions of 1 to spectra of galaxies with $\text{H}\alpha$ escape fractions less than 1. The $\text{H}\alpha$ and $\text{H}\beta$ lines in the spectra must be masked or replaced with continuum values. The literature relation is technically $f_{\text{esc}}(\text{H}\alpha) = f_{\text{esc}}(0.66\ \mu\text{m})^{2.3}$. Calzetti (1997b) uses the Milky Way extinction formula of Howarth (1983) to determine $\text{H}\alpha$ escape fractions for low-redshift dust-poor galaxies; if we instead use the attenuation formula, we get $f_{\text{esc}}(\text{H}\alpha) = f_{\text{esc}}(0.66\ \mu\text{m})^{2.1}$.

Our hypothesis is that the $\text{H}\alpha$ and $0.66\ \mu\text{m}$ escape fractions agree—that dusty galaxies have uniform dust distributions. Our method for determining $\text{H}\alpha$ escape fractions is nonstandard; we lack $\text{H}\beta$ luminosities for the $z \sim 1$ dusty galaxies. We first apply it to a sample of low-redshift dust-poor galaxies with the aim of reproducing the Calzetti (1997b) result.

3.1. Reproducing the relation between escape fractions for dust-poor galaxies

The sample, from Overzier et al. (2011), contains galaxies that lie roughly on the low-redshift IRX- β relation. This relation is a blunt instrument we use to determine whether or not galaxies obey an attenuation formula at UV wavelengths; $f_{\text{esc}}(0.16\ \mu\text{m})$ is a function of IRX and an attenuation formula relates $f_{\text{esc}}(0.16\ \mu\text{m})$ to β . Since these galaxies lie on the relation, we expect them to have dust properties that conform with the properties of the galaxies in the Calzetti et al. (2000) sample. We calculate $f_{\text{esc}}(\text{H}\alpha)$ and $f_{\text{esc}}(0.16\ \mu\text{m})$ for each galaxy in the following way.

- $f_{\text{esc}}(0.16\ \mu\text{m}) = (L_{\text{IR}}/(1.68 \times 0.16 \times L_{0.16}) + 1)^{-1}$. This is equivalent to $f_{\text{esc}}(0.16\ \mu\text{m}) = (\text{emergent UV SFR})/(\text{IR SFR} + \text{emergent UV SFR})$.
- Following the assumptions in 2.2.3: $f_{\text{esc}}(\text{H}\alpha) =$

(emergent $H\alpha$ SFR)/(IR SFR + emergent UV SFR).

We use these quantities to find, for the sample, a best-fit power-law index q for the form $f_{\text{esc}}(H\alpha) = f_{\text{esc}}(0.16 \mu\text{m})^q$.

The top left panel of Fig. 1 shows that $f_{\text{esc}}(H\alpha) = f_{\text{esc}}(0.16 \mu\text{m})^{0.80}$ for the low-redshift dust-poor galaxies. If we use the IR and UV luminosities from Overzier et al. 2011, $f_{\text{esc}}(H\alpha) = f_{\text{esc}}(0.16 \mu\text{m})^{0.84}$. We lack uncertainties on any SFRs so we also perform a robust linear regression, which requires a fit to the form $\log f_{\text{esc}}(H\alpha) = q \log f_{\text{esc}}(0.16 \mu\text{m})$. It returns a similar result, as does a bootstrap resampling. We recover a relation close to the Calzetti (1997b) relation for similar galaxies, so we have some confidence that our procedure is grossly correct. We stress, again, that there are no evolutionary connections between the low- and high-redshift galaxy samples; we aim only to reproduce the Calzetti (1997b) result with our nonstandard method of determining $f_{\text{esc}}(H\alpha)$.

3.2. A new relation for dusty galaxies at low redshift?

The top right panel of Fig. 1 shows that $f_{\text{esc}}(H\alpha) = f_{\text{esc}}(0.16 \mu\text{m})^{0.55}$ for the low-redshift dusty galaxies. We use uncertainties only on the emergent $H\alpha$ -derived SFR—we treat it as the dependent variable—in the weighted fit. The relation for dust-poor galaxies is seemingly inapplicable to dusty galaxies at low redshift. In §3.4 and 4 we explain why we preface ‘inapplicable’ with ‘seemingly.’

3.3. A corresponding relation for dusty galaxies at high redshift?

The bottom left panel of Fig. 1 shows that $f_{\text{esc}}(H\alpha) = f_{\text{esc}}(0.16 \mu\text{m})^{0.55}$ for high-redshift dusty galaxies. We leave limits out of this fit. The uncertainty in the index is very small; this is not surprising given the number of galaxies. The dispersion about the best-fit relation is large; the central 50% of galaxies with $H\alpha$ -detected SFRs lies between $f_{\text{esc}}(H\alpha) = f_{\text{esc}}(0.16 \mu\text{m})^{0.45}$ and $f_{\text{esc}}(H\alpha) = f_{\text{esc}}(0.16 \mu\text{m})^{0.66}$. A survival regression, which incorporates $H\alpha$ SFR limits in a fit to the form $\log f_{\text{esc}}(H\alpha) = q \log f_{\text{esc}}(0.16 \mu\text{m})$, finds $q = 0.47$, as does a simple linear regression using only the $H\alpha$ -detected SFRs. None of the galaxies have limits for both the UV and $H\alpha$ SFRs. The main effect of including limits in the regression is to increase the standard error of the sample’s best-fit index; a marginally different index is a secondary effect. Table 1 summarizes the relevant quantities for the main fit to each sample of galaxies.

3.4. Issues with the regressions

The escape fraction relations of dusty galaxies are subject to selection effects. The best-fit relation for the low-redshift dusty galaxies seems to: (1) underestimate $H\alpha$ escape fractions at low UV escape fractions; and (2) overestimate $H\alpha$ escape fractions at high UV escape fractions (top right panel of Fig. 1). This may reflect our constraint that $f_{\text{esc}}(H\alpha) = 1$ when $f_{\text{esc}}(0.16 \mu\text{m}) = 1$, but the lack of galaxies with $H\alpha$ escape fractions at or below the relation may be due to galaxies with $H\alpha$ SFRs below the limit of the sample. We do not measure $H\alpha$ line flux limits for galaxies that meet the selection criteria of Hwang & Geller (2013) and have undetected $H\alpha$ line

fluxes. If we replace all $H\alpha$ -detected SFRs with SFRs corresponding to the minimum $H\alpha$ line flux of the sample, we fill in the space around the relation.

High-redshift dusty galaxies with UV escape fractions $< 10^{-2}$ seem to have less dispersion in their $H\alpha$ escape fractions than do galaxies with UV escape fractions $> 10^{-2}$. Despite our best efforts to measure $H\alpha$ line flux limits, we still lack them for galaxies lacking spectroscopic redshifts. If we replace all $H\alpha$ -detected SFRs with SFRs corresponding to a reasonable $H\alpha$ line flux limit for the grism observations ($5 \times 10^{-17} \text{ erg s}^{-1} \text{ cm}^{-2}$), we fill in the space with low $H\alpha$ escape fractions at low UV escape fractions. The decrease in dispersion is probably an artifact of the grism detection limit and a paucity of spectroscopic redshifts in UDS and the part of COSMOS in CANDELS.

4. DISCUSSION

If we assume that dusty galaxies: (1) obey the Calzetti et al. (2000) attenuation formula; and (2) were to all have the same UV spectrum in the absence of dust; our results indicate that their $H\alpha$ and $0.66 \mu\text{m}$ escape fractions disagree. Unlike low-redshift dust-poor galaxies, dusty galaxies have $f_{\text{esc}}(H\alpha) = f_{\text{esc}}(0.66 \mu\text{m})^{1.6}$; like low-redshift dust-poor galaxies, dusty galaxies have nonuniform dust distributions. The relations between $f_{\text{esc}}(H\alpha)$ and $f_{\text{esc}}(0.66 \mu\text{m})$ are similar to those found by Onodera et al. (2010), Kashino et al. (2013), Price et al. (2013), and Reddy et al. (2015) and conflict with those of Erb et al. (2006). These studies assume the applicability of the Calzetti et al. (2000) attenuation formula, and use samples of high-redshift galaxies that are not necessarily dusty. Their UV escape fractions come from stellar population modeling, while ours come from IRX; their $H\alpha$ escape fractions come from ratios of averaged $H\alpha$ to averaged $H\beta$ luminosities, or ratios of $H\alpha$ to UV luminosities, while ours come from assumptions about SFRs.

However, dusty galaxies may disobey the Calzetti et al. (2000) attenuation formula, which complicates our interpretation of the more basic relation between UV and $0.66 \mu\text{m}$ escape fractions—the relation between escape fractions for just the regions with nonionizing UV-emitting stars (Reddy et al. 2010, 2012, 2015; Buat et al. 2011, 2012; Penner et al. 2012; Kriek & Conroy 2013). The true attenuation formula for dusty galaxies may have a higher $0.66 \mu\text{m}$ escape fraction for a given UV escape fraction than does the Calzetti et al. (2000) formula. A formula modified according to Kriek & Conroy (2013) with $\delta = -0.2$ and no bump at $0.2175 \mu\text{m}$ has $f_{\text{esc}}(0.66 \mu\text{m}) = f_{\text{esc}}(0.16 \mu\text{m})^{0.25}$ instead of $f_{\text{esc}}(0.66 \mu\text{m}) = f_{\text{esc}}(0.16 \mu\text{m})^{0.33}$. The combination of this Kriek & Conroy (2013) formula and our result implies that $f_{\text{esc}}(H\alpha) = f_{\text{esc}}(0.66 \mu\text{m})^{2.2}$. The (Reddy et al. 2015) attenuation formula has $f_{\text{esc}}(0.66 \mu\text{m}) = f_{\text{esc}}(0.16 \mu\text{m})^{0.23}$, implying that $f_{\text{esc}}(H\alpha) = f_{\text{esc}}(0.66 \mu\text{m})^{2.4}$. If the true formula instead has a much lower $0.66 \mu\text{m}$ escape fraction for a given UV escape fraction than does the Calzetti et al. (2000) formula—say, $f_{\text{esc}}(0.66 \mu\text{m}) = f_{\text{esc}}(0.16 \mu\text{m})^{0.55}$ —we conclude that for dusty galaxies the $H\alpha$ and $0.66 \mu\text{m}$ escape fractions agree. Our conclusion regarding the uniformity of dust distributions depends on the assumed

Table 1
Summary of regressions

Sample	q	Std. error of q	Residual std. error	DOF
Low-z dust-poor	0.799	0.094	6.0	13
Low-z dusty	0.548	0.029	67.0	54
High-z dusty	0.549	0.008	6.6	320

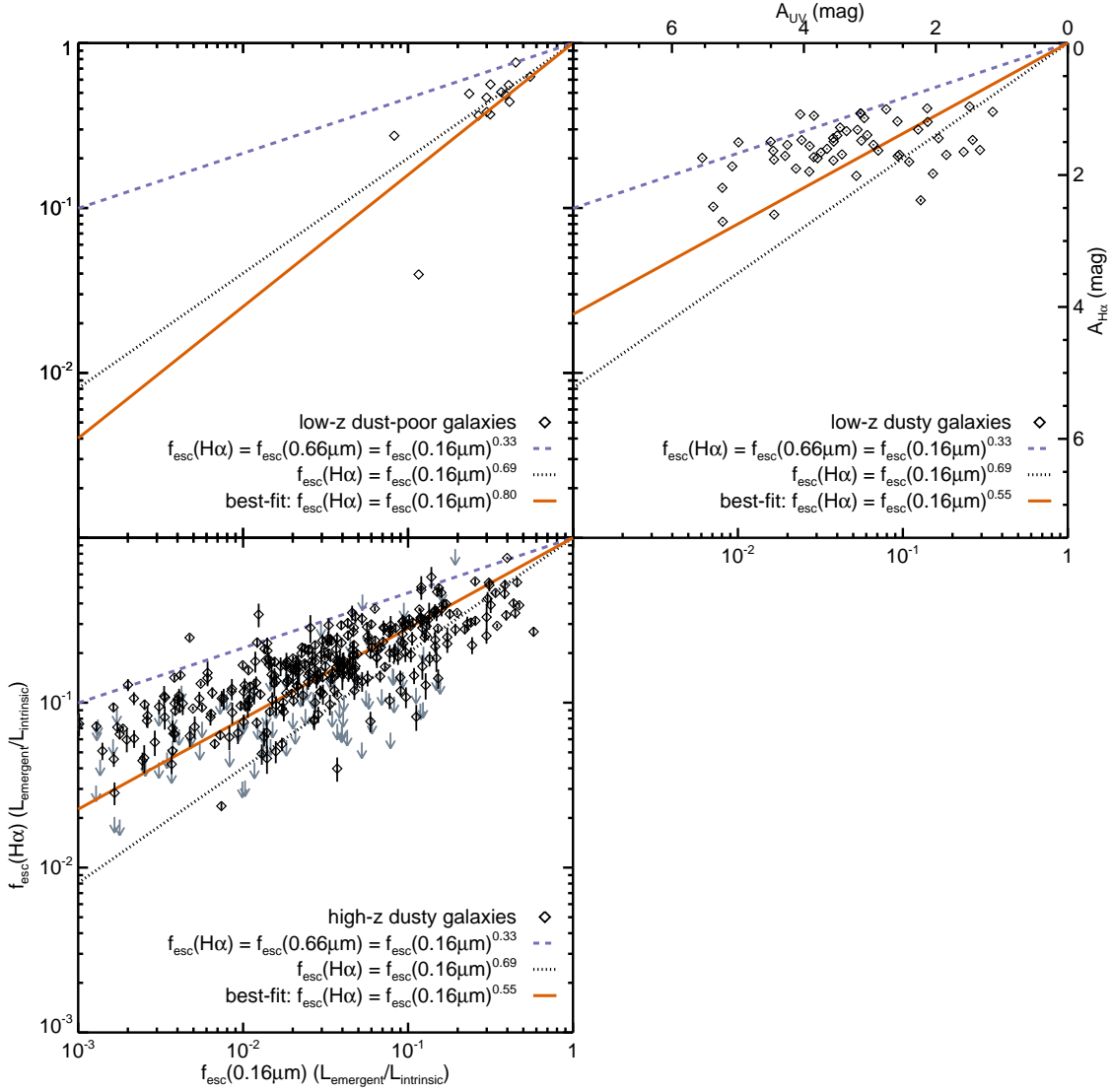


Figure 1. *Top left:* The H α escape fraction, $f_{\text{esc}}(\text{H}\alpha)$, as a function of the UV escape fraction, $f_{\text{esc}}(0.16\ \mu\text{m})$, for the low-redshift dust-poor galaxies. The dashed purple line shows $f_{\text{esc}}(0.66\ \mu\text{m})$, the extrapolation of $f_{\text{esc}}(0.16\ \mu\text{m})$ to the wavelength of H α using the Calzetti et al. (2000) attenuation formula, as a function of $f_{\text{esc}}(0.16\ \mu\text{m})$. This is the uniform dust distribution hypothesis for this attenuation formula. Calzetti (1997b), who study another sample of low-redshift dust-poor galaxies, find that H α escape fractions are lower than this extrapolation (dotted black line). We find a similar result (solid orange line). We have some confidence that our H α escape fractions are grossly correct. *Top right:* $f_{\text{esc}}(\text{H}\alpha)$ as a function of $f_{\text{esc}}(0.16\ \mu\text{m})$ for the low-redshift dusty galaxies. In low-redshift dusty galaxies, regions with ionizing stars have lower escape fractions than the extrapolation and higher escape fractions than they would have in low-redshift dust-poor galaxies. *Bottom left:* $f_{\text{esc}}(\text{H}\alpha)$ as a function of $f_{\text{esc}}(0.16\ \mu\text{m})$ for the high-redshift dusty galaxies. In high-redshift dusty galaxies, regions with ionizing stars have lower escape fractions than the extrapolation and higher escape fractions than they would have in low-redshift dust-poor galaxies. A conclusion about the uniformity of dust distributions in high-redshift dusty galaxies is subject to an assumption about the attenuation formula.

attenuation formula. We cannot reject our hypothesis. The Calzetti et al. (2000) formula does demarcate the upper boundary of $f_{\text{esc}}(\text{H}\alpha)$ for the high-redshift dusty

galaxies (bottom left panel of Fig. 1), so if it is the true formula then at least some dusty galaxies have uniform dust distributions. The unambiguous statement

we make is that dusty galaxies have relations between $H\alpha$ and UV escape fractions that are different from the relation for low-redshift dust-poor galaxies.

The dispersion about the best-fit relation for high-redshift dusty galaxies is large, yet it is susceptible to our possibly invalid assumption that a galaxy’s instantaneous SFR has, for at least 10^8 yr, equaled its prolonged SFR. For example, if most massive stars formed over 15 Myr instead of 300 Myr, we should multiply $L_{0.16}$ and L_{IR} by larger numbers than we do here to derive the UV and IR SFRs. The true UV SFR is 57% higher and the true IR SFR is 63% higher (Madau & Dickinson 2014). The true UV escape fraction is little different; because the true total SFR is higher, the true $H\alpha$ escape fraction is lower. Another scenario is that massive stars stopped forming within the last 15 Myr. Perhaps some of the high-redshift dusty galaxies have complicated star formation histories; the combined effect of deriving correct SFRs might lead to lower dispersion.

There are few ways to resolve the uncertainties regarding star formation histories and the applicability of the Calzetti et al. (2000) attenuation formula to dusty galaxies. One (partial) way is to use the formula and $f_{\text{esc}}(H\alpha)$ to predict the escape fraction of the $H\beta$ luminosity, $f_{\text{esc}}(H\beta)$. The ratio of intrinsic $H\alpha$ to $H\beta$ luminosities is 2.86 under reasonable assumptions; with $H\beta$ observations, we can use $(L_{H\alpha}/L_{H\beta})/2.86 = f_{\text{esc}}(H\alpha)/f_{\text{esc}}(H\beta)$ and from this determine $f_{\text{esc}}(H\beta)$. If the predicted and determined $H\beta$ escape fractions agree, the assumed attenuation formula is probably valid at optical wavelengths; the assumed star formation histories are also probably valid. The histories are valid because the prediction is history-dependent and the determination is history-independent—both line luminosities are from ionized gas surrounding the same stars. If the predicted and determined fractions disagree, the attenuation formula at optical wavelengths can be different for dusty galaxies or their true $f_{\text{esc}}(H\alpha)$ can be different. The formula can differ due to dust not distributed as a uniform foreground screen; see table 1 and fig. 3b of Calzetti 2001. Fig. 2 shows this test applied to the low-redshift dusty galaxies. To apply this test to high-redshift dusty galaxies, we need near-IR spectra that cover the $H\beta$ line. If the dispersion of $H\alpha$ escape fractions at a given UV escape fraction for high-redshift dusty galaxies remains, there must be a diversity of dust distributions. Either way, this test provides no information on the relation between UV and $0.66\ \mu\text{m}$ escape fractions; more extrapolations are necessary to definitively interpret Fig. 1.

5. SUMMARY

1. We measure $H\alpha$ line luminosities and limits, from *HST*/WFC3-IR grism spectra, for $z \sim 1$ galaxies with detected $100\ \mu\text{m}$ emission. We determine rest-frame UV continuum power-law indices (β values) and ratios of IR to UV luminosities (IRX values).
2. For each galaxy we determine $f_{\text{esc}}(0.16\ \mu\text{m})$, the escape fraction at $0.16\ \mu\text{m}$, from IRX. We determine $f_{\text{esc}}(H\alpha)$, the $H\alpha$ escape fraction, from the $H\alpha$ luminosity and the total star formation rate.
3. For the Overzier et al. (2011) sample of low-redshift dust-poor galaxies, we recover the Calzetti

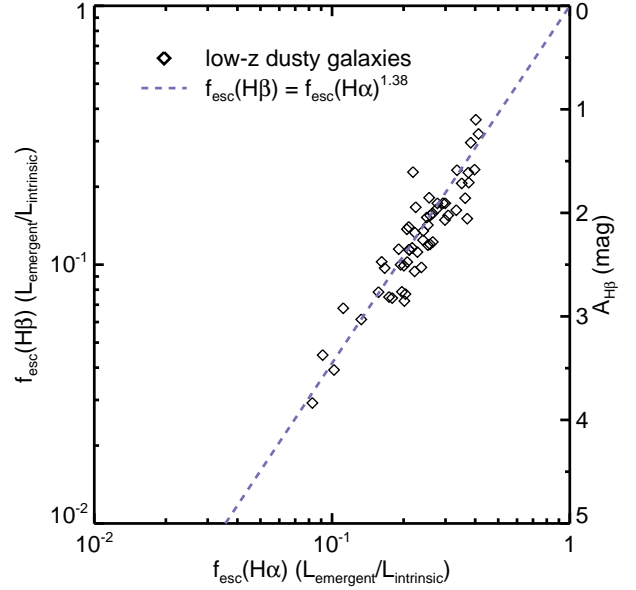


Figure 2. $H\beta$ escape fraction, $f_{\text{esc}}(H\beta)$, as a function of $H\alpha$ escape fraction, $f_{\text{esc}}(H\alpha)$, for the low-redshift dusty galaxies. We determine $f_{\text{esc}}(H\beta)$ using $f_{\text{esc}}(H\alpha)$ and the ratios of $H\alpha$ and $H\beta$ luminosities. The Calzetti et al. (2000) attenuation formula has $f_{\text{esc}}(H\beta) = f_{\text{esc}}(H\alpha)^{1.38}$ (dashed purple line). If $H\beta$ measurements of high-redshift dusty galaxies agree with the prediction, we can resolve uncertainties related to star formation histories and the validity of the Calzetti et al. (2000) attenuation formula at optical wavelengths; otherwise, we might not.

(1997b) relation between $H\alpha$ and UV escape fractions: $f_{\text{esc}}(H\alpha) = f_{\text{esc}}(0.16\ \mu\text{m})^{0.80}$. Our nonstandard method for determining $H\alpha$ escape fractions should be grossly correct.

4. For the Hwang & Geller (2013) sample of low-redshift dusty galaxies, we find that $f_{\text{esc}}(H\alpha) = f_{\text{esc}}(0.16\ \mu\text{m})^{0.55}$.
5. For our sample of dusty galaxies at $0.7 < z < 1.5$, we find that $f_{\text{esc}}(H\alpha) = f_{\text{esc}}(0.16\ \mu\text{m})^{0.55}$. The dispersion about the best-fit relation is large.
6. The interpretation of the results for dusty galaxies is unclear. If we assume that the Calzetti et al. (2000) attenuation formula applies to these galaxies, our results agree with those of Onodera et al. (2010), Kashino et al. (2013), Price et al. (2013), and Reddy et al. (2015) and conflict with those of Erb et al. (2006): $f_{\text{esc}}(H\alpha) = f_{\text{esc}}(0.66\ \mu\text{m})^{1.6}$. They study samples comprising dust-poor and dusty galaxies. Dusty galaxies have nonuniform dust distributions. However, dusty galaxies may disobey the Calzetti et al. (2000) attenuation formula.
7. Measurements of the ratios of $H\alpha$ to $H\beta$ luminosities may decrease the dispersion in the relation between $H\alpha$ and UV escape fractions for dusty galaxies at $z \sim 1$. If the dispersion is real, these galaxies have diverse dust distributions.

ALMA is beginning to produce images of the dust distributions in high-redshift galaxies. These images lead to

direct tests, independent of the attenuation formula, of the uniform screen assumption. They also have the potential to reveal the parts of galaxies that may never be detected at UV and optical wavelengths: surprises surely abound.

REFERENCES

- Balestra, I., Mainieri, V., Popesso, P., et al. 2010, *A&A*, 512, AA12
- Boissier, S., Boselli, A., Buat, V., Donas, J., & Milliard, B. 2004, *A&A*, 424, 465
- Brammer, G. B., van Dokkum, P. G., Franx, M., et al. 2012, *ApJS*, 200, 13
- Buat, V., Noll, S., Burgarella, D., et al. 2012, *A&A*, 545, A141
- Buat, V., Giovannoli, E., Heinis, S., et al. 2011, *A&A*, 533, A93
- Calzetti, D. 2001, *PASP*, 113, 1449
- Calzetti, D., Armus, L., Bohlin, R. C., et al. 2000, *ApJ*, 533, 682
- Calzetti, D. 1997b, *American Institute of Physics Conference Series*, 408, 403
- Calzetti, D. 1997a, *AJ*, 113, 162
- Calzetti, D., Kinney, A. L., & Storchi-Bergmann, T. 1994, *ApJ*, 429, 582
- Chary, R., & Elbaz, D. 2001, *ApJ*, 556, 562
- Díaz-Santos, T., Charmandaris, V., Armus, L., et al. 2010, *ApJ*, 723, 993
- Donley, J. L., Koekemoer, A. M., Brusa, M., et al. 2012, *ApJ*, 748, 142
- Erb, D. K., Steidel, C. C., Shapley, A. E., et al. 2006, *ApJ*, 647, 128
- Fadda, D., Yan, L., Lagache, G., et al. 2010, *ApJ*, 719, 425
- Galametz, A., Grazian, A., Fontana, A., et al. 2013, *ApJS*, 206, 10
- Guo, Y., Ferguson, H. C., Giavalisco, M., et al. 2013, *ApJS*, 207, 24
- Howarth, I. D. 1983, *MNRAS*, 203, 301
- Hwang, H. S., & Geller, M. J. 2013, *ApJ*, 769, 116
- Juneau, S., Dickinson, M., Bournaud, F., et al. 2013, *ApJ*, 764, 176
- Kashino, D., Silverman, J. D., Rodighiero, G., et al. 2013, *ApJ*, 777, L8
- Kauffmann, G., Heckman, T. M., Tremonti, C., et al. 2003, *MNRAS*, 346, 1055
- Kennicutt, R., 1999, *ARA&A*, 36, 189
- Kriek, M., & Conroy, C. 2013, *ApJ*, 775, L16
- Kurk, J., Cimatti, A., Daddi, E., et al. 2013, *A&A*, 549, AA63
- Le Fèvre, O., Vettolani, G., Paltani, S., et al. 2004, *A&A*, 428, 1043
- Lilly, S. J., Le Brun, V., Maier, C., et al. 2009, *ApJS*, 184, 218
- Liu, G., Calzetti, D., Hong, S., et al. 2013, *ApJ*, 778, L41
- Madau, P., & Dickinson, M. 2014, arXiv:1403.0007
- Magnelli, B., Popesso, P., Berta, S., et al. 2013, *A&A*, 553, A132
- Ménard, B., Scranton, R., Fukugita, M., & Richards, G. 2010, *MNRAS*, 405, 1025
- Mignoli, M., Cimatti, A., Zamorani, G., et al. 2005, *A&A*, 437, 883
- Muñoz-Mateos, J. C., Gil de Paz, A., Boissier, S., et al. 2009, *ApJ*, 701, 1965
- Onodera, M., Arimoto, N., Daddi, E., et al. 2010, *ApJ*, 715, 385
- Overzier, R. A., Heckman, T. M., Wang, J., et al. 2011, *ApJ*, 726, L7
- Overzier, R. A., Heckman, T. M., Tremonti, C., et al. 2009, *ApJ*, 706, 203
- Penner, K., Dickinson, M., Pope, A., et al. 2012, *ApJ*, 759, 28
- Prescott, M. K. M., Kennicutt, R. C., Jr., Bendo, G. J., et al. 2007, *ApJ*, 668, 182
- Price, S. H., Kriek, M., Brammer, G. B., et al. 2014, *ApJ*, 788, 86
- Ravikumar, C. D., Puech, M., Flores, H., et al. 2007, *A&A*, 465, 1099
- Reddy, N. A., Kriek, M., Shapley, A. E., et al. 2015, arXiv:1504.02782
- Reddy, N., Dickinson, M., Elbaz, D., et al. 2012, *ApJ*, 744, 154
- Reddy, N. A., Erb, D. K., Pettini, M., Steidel, C. C., & Shapley, A. E. 2010, *ApJ*, 712, 1070
- Santini, P., Ferguson, H. C., Fontana, A., et al. 2014, arXiv:1412.5180
- Simpson, C., Rawlings, S., Ivison, R., et al. 2012, *MNRAS*, 421, 3060
- Simpson, J. M., Smail, I., Swinbank, A. M., et al. 2015, *ApJ*, 799, 81
- Szokoly, G. P., Bergeron, J., Hasinger, G., et al. 2004, *ApJS*, 155, 271
- Vanzella, E., Cristiani, S., Dickinson, M., et al. 2008, *A&A*, 478, 83
- Weiner, B. J., Papovich, C., Bundy, K., et al. 2007, *ApJ*, 660, L39
- Willman, B., Geha, M., Strader, J., et al. 2011, *AJ*, 142, 128
- Willman, B., Blanton, M. R., West, A. A., et al. 2005, *AJ*, 129, 2692
- Yamada, T., Kodama, T., Akiyama, M., et al. 2005, *ApJ*, 634, 861
- Younger, J. D., Fazio, G. G., Ashby, M. L. N., et al. 2010, *MNRAS*, 407, 1268
- Zaritsky, D. 1994, *AJ*, 108, 1619

Table 2
Measured and derived quantities for the sample at $z > 0.7$

RA, IR deg	Dec, IR deg	RA, opt. deg	Dec, opt. deg	z	β	σ_β	$0.16 \times L_{0.16}$ L_\odot	$\sigma_{L_{0.16}}$ L_\odot	$L_{\text{H}\alpha}$ L_\odot	$\sigma_{L_{\text{H}\alpha}}$ L_\odot	$L_{\text{H}\alpha}$ lim. L_\odot	L_{IR} L_\odot	$\sigma_{L_{\text{IR}}}$ L_\odot
GOODS-S													
53.113487	-27.933195	53.113470	-27.933294	1.098 ^G	0.53	0.34	1.1e+10	4.9e+08	5.6e+08	2.1e+07	...	6.2e+11	1.9e+10
53.096371	-27.925898	53.096385	-27.925972	1.146	-1.89	0.41	7.9e+09	3.3e+08	3.3e+08	2.6e+07	...	2.2e+11	4.9e+10
53.090958	-27.922218	53.090977	-27.922288	1.390	1.41	0.48	8.4e+08	4.5e+08	3.1e+08	2.2e+07	...	5.5e+11	2.7e+10
53.184750	-27.920420	53.184801	-27.920432	0.953	-1.68	0.15	1.2e+10	3.9e+08	1.6e+08	2.3e+07	...	9.3e+10	1.7e+07
53.104836	-27.913826	53.104830	-27.913926	1.090	0.61	0.61	3.5e+09	2.7e+08	1.2e+08	1.7e+07	...	1.8e+11	6.2e+09

Note. — Columns: RA and Dec, IR, are positions in the *Herschel* catalogs. They are based on positions of *Spitzer*/IRAC priors. RA and Dec, opt., are positions in the CANDELS catalogs. $L_{\text{H}\alpha}$ lim. is a 5σ upper limit to the H α line luminosity. The entire table is published in the electronic edition of ApJ. A portion is shown here for guidance regarding its form and content.

^G Spectroscopic redshift solely from grism observations.

Table 3
Measured and derived quantities for the samples at $z < 0.2$

RA deg	Dec deg	z	β	σ_β	$0.16 \times L_{0.16}$ L_\odot	$\sigma_{L_{0.16}}$ L_\odot	$L_{H\beta}$ L_\odot	$\sigma_{L_{H\beta}}$ L_\odot	$L_{H\alpha}$ L_\odot	$\sigma_{L_{H\alpha}}$ L_\odot	L_{IR} L_\odot	$\sigma_{L_{IR}}$ L_\odot
Dust-poor galaxies												
30.987125	-8.132919	0.189	-1.66	0.04	3.5e+10	2.9e+08	1.4e+08	...	4.6e+08	...	8.5e+10	1.8e+09
33.452250	12.997628	0.219	-0.45	0.05	4.3e+10	4.3e+08	3.6e+07	...	1.4e+08	...	5.4e+11	3.0e+09
52.191625	1.197458	0.142	-1.68	0.04	1.9e+10	1.7e+08	7.4e+07	...	2.4e+08	...	5.4e+10	1.0e+09
59.391667	-5.622139	0.204	-1.28	0.06	2.9e+10	3.5e+08	9.4e+07	...	3.5e+08	...	1.1e+11	1.9e+09
125.007167	50.844211	0.217	-1.55	0.08	2.6e+10	4.0e+08	2.4e+08	...	8.1e+08	...	4.8e+11	4.9e+09

Note. — The entire table is published in the electronic edition of ApJ. A portion is shown here for guidance regarding its form and content.